Alignment of the CMS Muon System with Tracks

J. Pivarski
Department of Physics, Texas A&M University 77843, USA and
The CMS Collaboration

As its name suggests, the Compact Muon Solenoid (CMS) features a full tracking spectrometer for identifying and measuring the momenta of muons. Every muon passes through 18–44 layers, providing a highly redundant track capable of validating and improving the momentum measurement from the CMS silicon tracker. But like any tracking system, its performance depends on precise knowledge of the positions of the tracking elements relative to one another and relative to the tracker. We present methods to align the muon system with tracks and the performance of these algorithms using cosmic rays and beam-halo data from the 2008 run of the LHC.

1. Introduction

The Compact Muon Solenoid (CMS) experiment [1] is designed to explore physics at the TeV energy scale, exploiting proton-proton collisions delivered by the Large Hadron Collider (LHC) [2]. Muons provide a particularly useful probe of new phenomena, in that many signatures of new physics and few QCD-related backgrounds yield energetic muons. A primary component of the CMS design, therefore, is a large muon tracking system with excellent muon efficiency and background rejection [3].

Data from the muon system also contribute to the muon momentum resolution, particularly for the most energetic muons. The trajectories of highly energetic muons have small curvature in the magnetic field, and the large distance of muon detectors from the LHC beamline (up to 7 m) help to resolve the curvature, and therefore the transverse momentum (p_T) of the muons. However, the spatial resolution on which this momentum measurement depends requires the locations of muon system components to be well known; in other words, the muon system must be well aligned. The relevance of muon system alignment for a sample physics signature ($Z' \to \mu\mu$) is illustrated in Fig. 1.

The muon system is composed of hundreds of modular tracking chambers, each containing 6–12 measurement layers. Drift tube (DT) chambers are arranged in a barrel geometry around the beamline, while Cathode Strip Chambers (CSC) are oriented in endcap rings on both sides of the collision point. Muons traversing each chamber are reconstructed as linear track segments, and these are combined with tracks in the central CMS silicon tracker to form global muon tracks which span the entire detector.

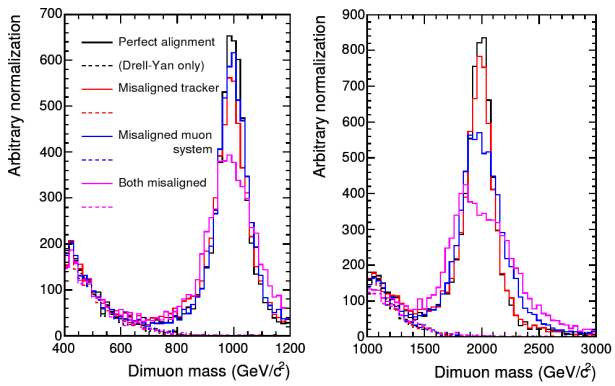

Figure 1: Reconstructed dimuon mass for hypothetical 1 TeV (left) and 2 TeV (right) Z' bosons, under different assumptions of tracker and muon system misalignment.

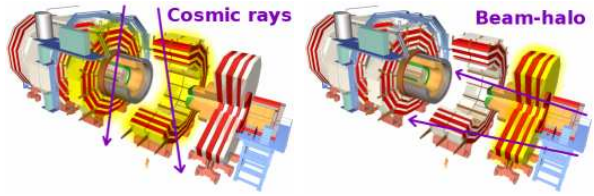

Figure 2: Illustration of the CMS detector, highlighting the barrel (left) and the endcap (right). Cosmic ray muons are better probes of barrel alignment and beam-halo muons are better probes of endcap alignment due to the orthogonality to the respective detector measurement planes.

Alignment techniques have been developed to determine the positions and orientations of the muon chambers by correcting systematic biases in the distributions of tracks and local track segments. While these techniques were designed primarily for alignment using muons from proton collisions, they have been successfully applied to cosmic rays and beam-halo muons from the 2008 LHC beam circulation tests (see Fig. 2).

This paper presents the techniques and their results using pre-collisions data. The technique described in the Section 2 aligns each chamber relative to the CMS tracker using tracker tracks, and it is demonstrated using cosmic rays that traverse the muon barrel and the tracker. Section 3 presents a technique for aligning CSC chambers within endcap rings with much smaller event samples, and it is demonstrated using muons from a 9-minute single-beam run of the LHC.

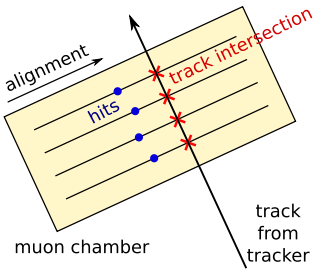

Figure 3: Cartoon of a misaligned muon chamber: misalignment is inferred from a systematic bias in the hits-minus-track intersection distribution.

2. Alignment relative to the CMS tracker with cosmic rays

The purpose of this procedure is to align all muon chambers in the same coordinate system as the CMS tracker. It will be used with collisions muons when large samples become available (tens of inverse picobarns), but cosmic ray datasets already collected have equivalent sample sizes for the top and bottom chambers of the central barrel of the muon system.

2.1. Method

The basic idea is to use tracks from the CMS tracker as a reference to position and orient each muon chamber. For this procedure, track parameters are determined using the tracker-only and are propagated through the magnetic field map and material distribution to the muon chambers, where they can be compared with the muon hits. Figure 3 illustrates the effect of a simple displacement in chamber position, in which muon measurements (hits) are offset from the extrapolated track. In a large sample, the distribution of residuals (hits minus track intersections with the measurement layers) has a systematic bias which can be inverted to derive and correct the misalignment.

In general, six rigid-body alignment parameters— three translations and three rotations— must be determined from four component muon chamber residuals, two displacements (x and y) and two angles ($\frac{dx}{dz}$ and $\frac{dy}{dz}$); see Fig. 4. Estimators for the alignment corrections are derived from a residuals dataset through the Jacobian of the transformation between the 4-dimensional residuals space and the 6-dimensional alignment correction space: a 6×4 matrix. Additional corrections for known propagation effects and potential magnetic field errors generalize the linear problem into one that can be solved by a non-linear fit. A sample fit result is presented in Figs. 5 and 6.

Large numbers of cosmic rays passing through the tracker are only available in the center of the barrel of the muon system. Therefore, the alignment was only applied using chambers from the central three wheels (modular transverse cross-sections of the muon system), excluding the two horizontal chambers on the left and right extremes of each wheel.

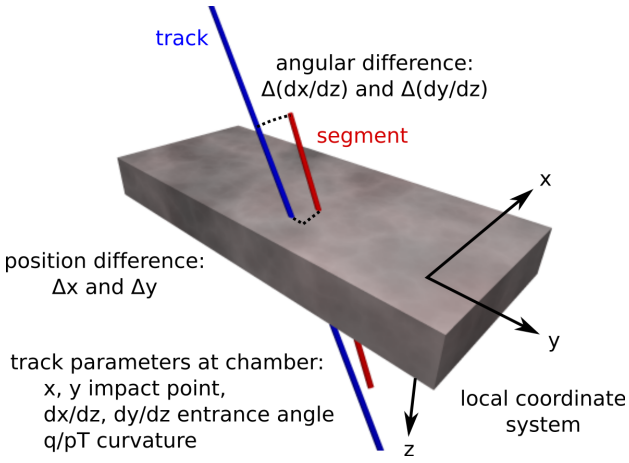

Figure 4: Definition of coordinates and 4-component residuals (two displacements and two angles).

2.2. Monte Carlo simulation

To verify that the procedure is working, a cosmic ray Monte Carlo sample was simulated with misaligned muon chambers. The alignment algorithm was applied to the simulated dataset and the real dataset with the same parameters. The simulation included all known detector effects except for misalignment of the tracker, misalignment of layers inside the chambers, and errors in the magnetic field map and material budget, which can affect aligned chamber positions but do not test the performance of the alignment algorithm itself.

Figure 7 presents the results of the test by comparing each aligned chamber parameter with the true value, known in simulation. The local x and ϕ_y coordinates determine the bending of tracks in the transverse plane and hence set the momentum scale. Their accuracies, 200 μm and 0.1 mrad, respectively, are approximately the scale of intrinsic hit resolutions (100–300 μm), and hence residual misalignment does not dominate the momentum resolution of high-energy muons.

2.3. Momentum resolution

Optimization of momentum resolution is a primary goal of alignment, but it can also serve as a cross-check. To measure the momentum resolution of tracks before and after muon chamber alignment, cosmic rays traversing the entire CMS detector were split close to the beamline and both halves were fitted indepen-

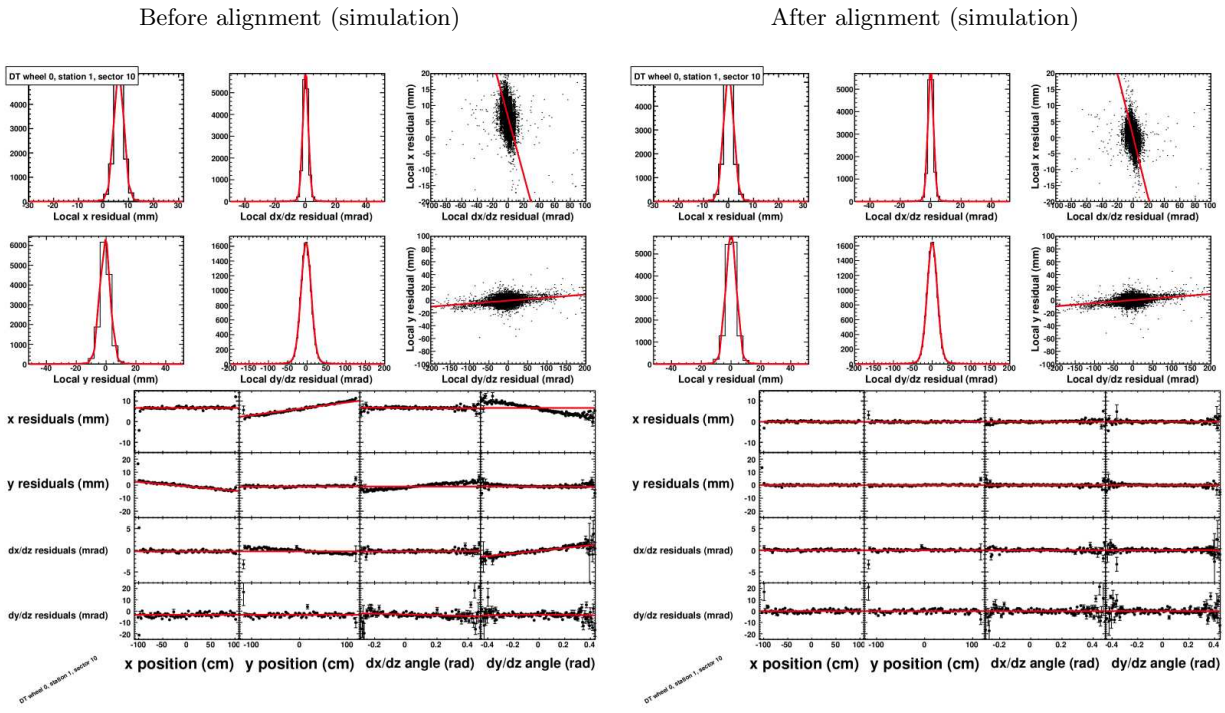

Figure 5: Example alignment fit from **simulated** cosmic rays (one chamber). Left and right groups of plots are before and after alignment, respectively. The six top histograms are each of the four residuals components and their correlations (detector effects). The bottom 16 are residuals versus position and entrance angle (misalignment).

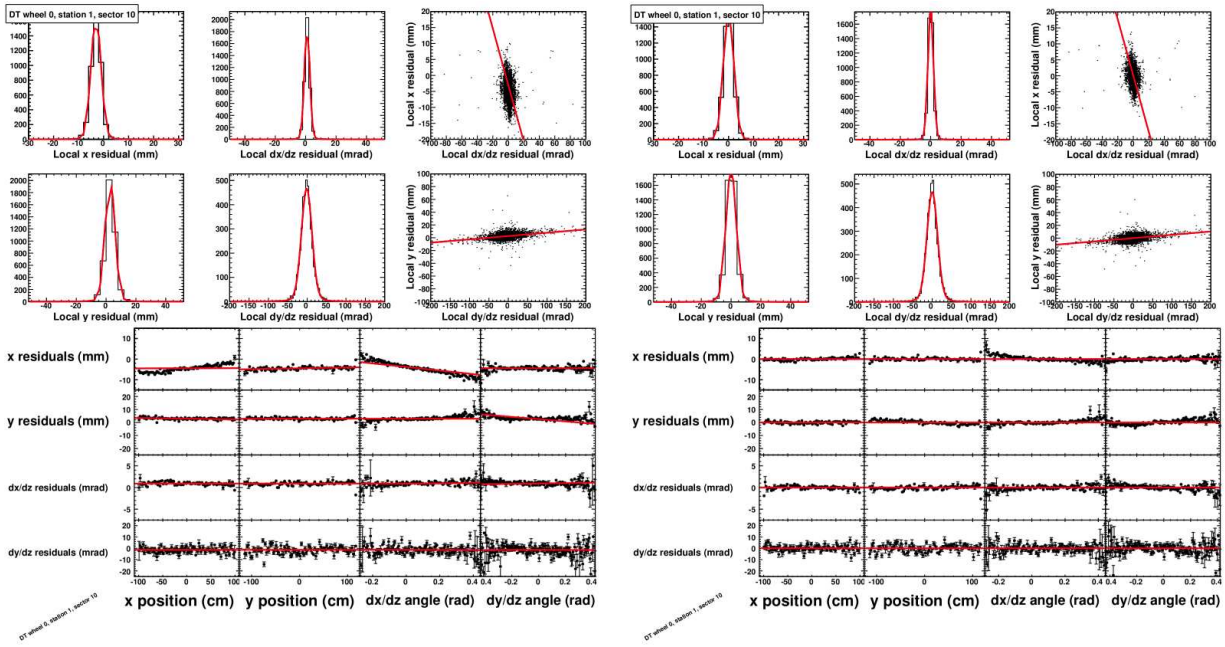

Figure 6: Example alignment fit from cosmic ray **data**. See Fig. 5 caption for details.

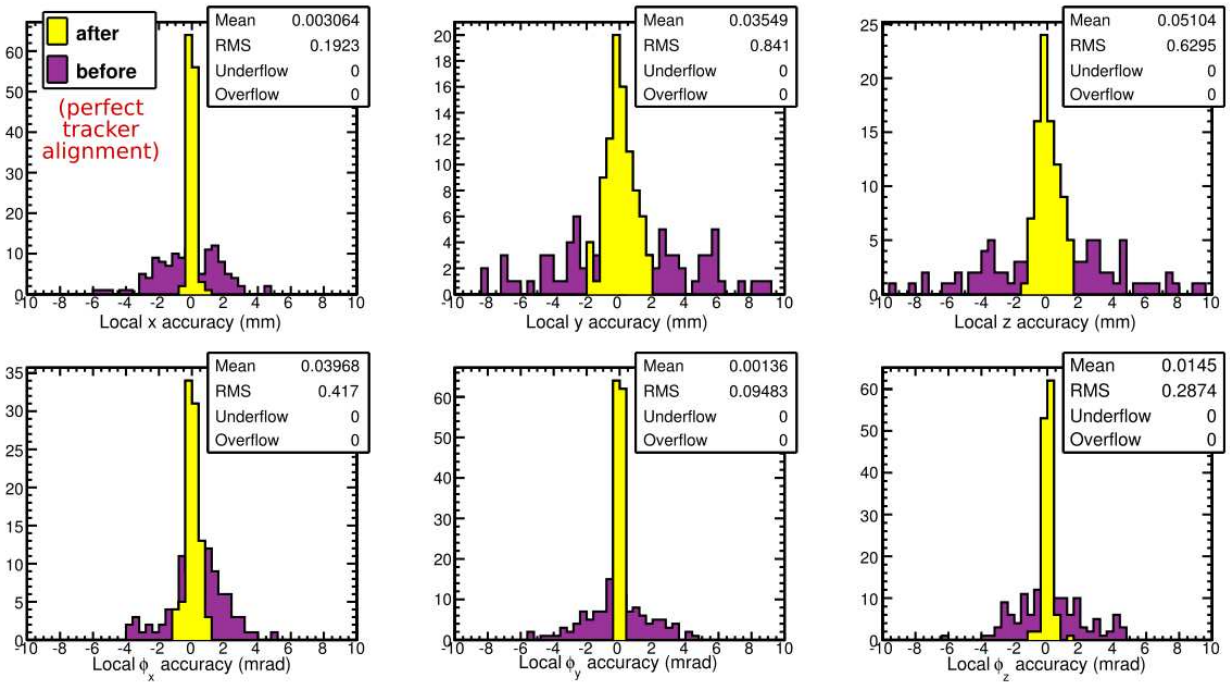

Figure 7: Histogram of aligned chamber parameters minus true chamber parameters for a simulated cosmic ray alignment challenge. To illustrate the performance of the alignment method itself, tracker misalignments were not considered.

dently. Any differences in track parameters between the top and bottom halves are purely instrumental.

Figure 8 presents the fractional curvature resolution, that is, differences in curvature (q/p_T, where q is the muon charge) between the top and bottom cosmic ray tracks divided by the curvature. Cosmic rays were required to have $p_T > 200$ GeV/c to increase sensitivity to muon misalignment. Results from several track-fitting procedures are presented: tracker-only (no muon hits), tracker with first muon station hits (innermost chambers only), before and after alignment. Including only the first muon station in track-fits reduces sensitivity to hit confusion from muon showers, prominent for muons of several hundred GeV/c. It also limits this cross-check to test the alignment of the first muon station.

For $p_T \approx 200$ GeV/c muons, tracker hits dominate the momentum resolution, but we can see the biasing effect of misalignment. Before alignment, track-fits including muon hits were biased because hit positions were misreconstructed with small quoted uncertainties (only the intrinsic hit uncertainties). The bias depends on which chambers the muons intersected, resulting in a broadening of the whole distribution. After alignment, the momentum distribution is narrower and more centered, reproducing the resolution of the tracker-only. The tracker-only fits are unaffected by the muon alignment, though the tracker-only distributions differ slightly between the two cases because more muons were identified after muon alignment.

3. Alignment of endcap rings with beam-halo muons

An alternate technique was used to align endcap CSC chambers using a small number of beam-halo tracks from the LHC beam circulation tests of 2008.

3.1. Method

CSC chambers overlap along the edges of their active area, such that muons passing through these overlap regions leave tracks in both chambers in each pair (left of Fig. 9). Uncertainties due to track propagation are negligible because the tracks are not propagated through large amounts of material. From the continuity and linearity of observed tracks, one can derive the relative positions of each pair of chambers, and propagate that information transitively around rings of mutually-overlapping chambers (right of Fig. 9). The resulting measurement is insensitive to the global position and orientation of each whole ring, but precisely interaligns the chambers within the rings.

Of the six rigid-body alignment parameters, this method is sensitive to $r\phi$ (rotation around the nominal beamline), ϕ_z (rotation in the measurement plane, which is perpendicular to the beamline), and ϕ_y (rotation around radial axes). These are illustrated for a typical CSC in Fig. 10.

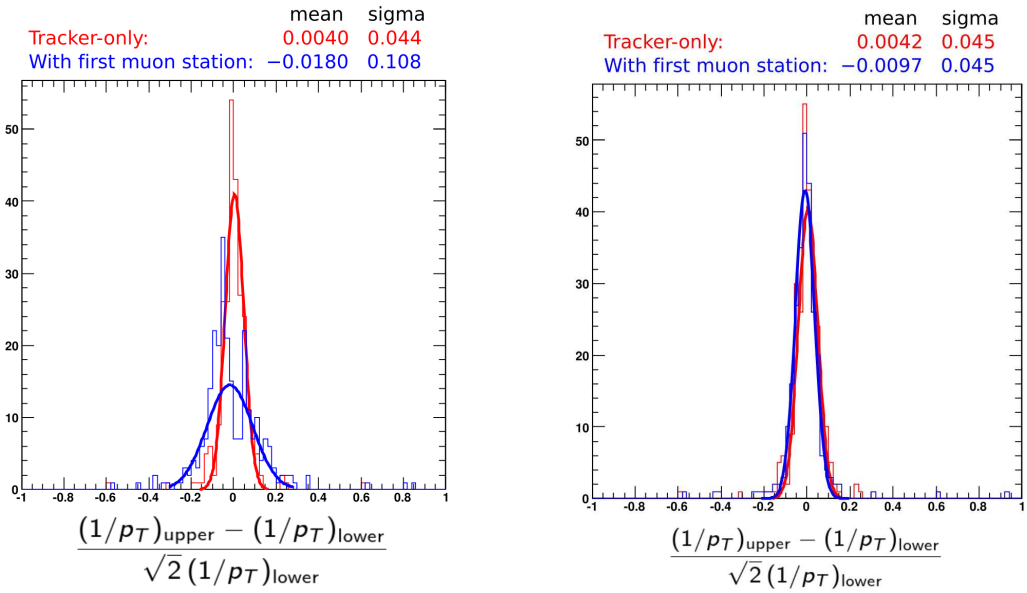

Figure 8: Curvature resolution for tracks ($p_T > 200$ GeV/c) including muon hits (blue) and not including muon hits (red), before alignment (left) and after alignment (right), derived from split cosmic ray tracks.

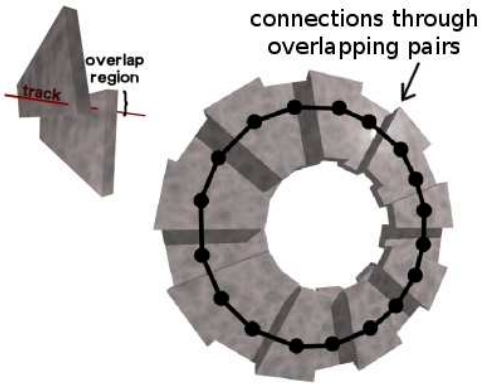

Figure 9: The local CSC alignment algorithm uses track segments passing through pairs of neighboring chambers to determine relative alignments, and builds a ring geometry by combining pairwise information in a single fit.

3.2. Monte Carlo simulation

A Monte Carlo simulation approximating LHC beam-halo conditions was used to test the procedure. The simulation was not intended to model the radial and azimuthal distribution of beam-halo muons from the LHC exactly, as these are notoriously difficult to predict, but provided a framework for testing the procedure with similar numbers of muons (33 000 in the overlap regions). Figure 11 demonstrates that the alignment algorithm successfully restores the correct alignment parameters from an initially misaligned system.

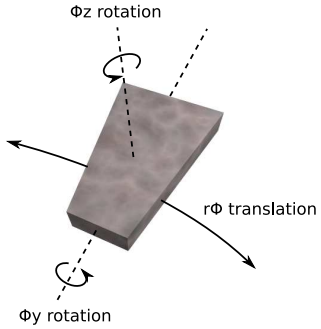

Figure 10: Three aligned coordinates of CSC chambers.

3.3. Alignment cross-checks

The alignment algorithm was applied using muons from the largest beam-halo dataset: a 9-minute circulation of the anti-clockwise LHC beam. These muons primarily illuminated rings close to the beamline and on the negative-z side of CMS, so rings ME−2/1 and ME−3/1 were chosen for alignment.

An independent alignment was performed using photogrammetry (measurement of photographs of the detector before it was fully assembled), which we use to verify the track-based method. In Fig. 12, differences between aligned and design ϕ_z angles are plotted from the track-based method and photogrammetry, in which we see a clear correlation. These comparisons are summarized by Fig. 13, in which differences in $r\phi$ positions and ϕ_z angles (the two parameters measurable by photogrammetry) between the two methods are histogrammed. Subtracting the photogrammetry uncertainty in quadrature from the RMS of these his-

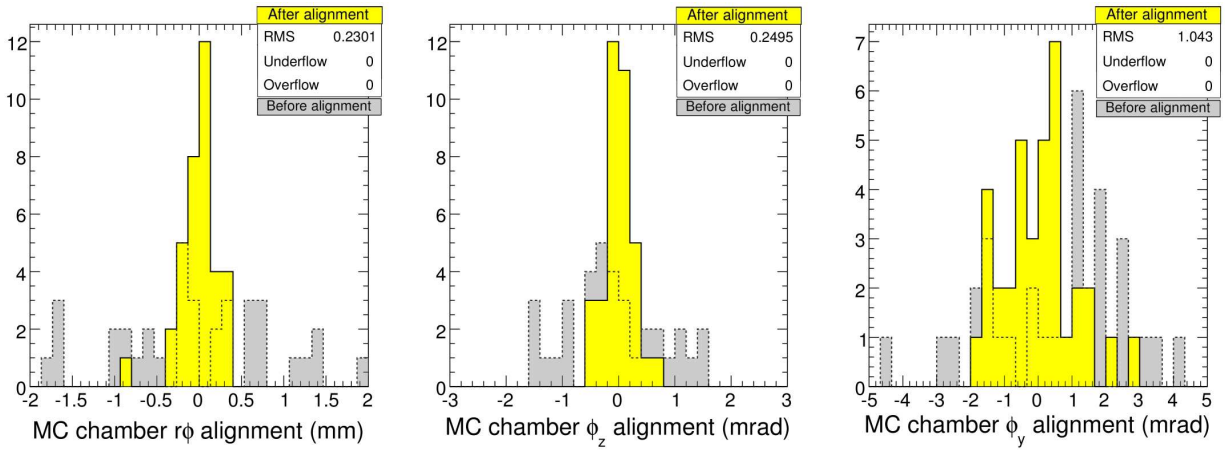

Figure 11: Histogram of aligned chamber parameters minus true chamber parameters for a simulated beam-halo alignment challenge.

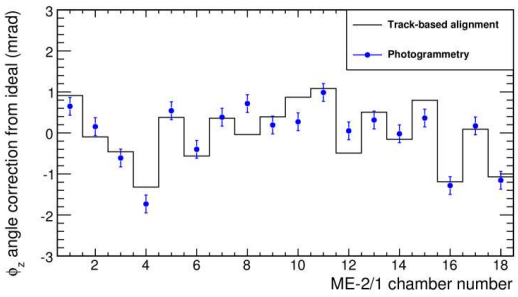

Figure 12: Alignment corrections for a sample ring from the track-based method and from a photograph of the detector, illustrating a strong correlation.

tograms, the track-based accuracy is 270 μm in $r\phi$ and 0.35 mrad in ϕ_z— on the scale of the intrinsic hit resolutions (100–300 μm).

4. Conclusions

Two track-based techniques were developed to align chambers in the CMS muon system. Both will be applied to muons from the first collisions of the LHC, but they were first applied to available cosmic ray and beam-halo data. Alignment was shown to significantly improve the momentum resolution of the central barrel DTs when aligned using high-statistics cosmic rays, and independent methods of aligning the inner-ring CSCs were shown to agree with high precision, despite the small numbers of available tracks. These tests demonstrate that CMS is ready to achieve a precise alignment of the muon system when LHC collisions become available, thereby optimizing high-energy muon resolution for discoveries at the TeV energy scale.

Acknowledgments

We thank the technical and administrative staff at CERN and other CMS Institutes, and acknowledge support from: FMSR (Austria); FNRS and FWO (Belgium); CNPq, CAPES, FAPERJ, and FAPESP (Brazil); MES (Bulgaria); CERN; CAS, MoST, and NSFC (China); COLCIENCIAS (Colombia); MSES (Croatia); RPF (Cyprus); Academy of Sciences and NICPB (Estonia); Academy of Finland, ME, and HIP (Finland); CEA and CNRS/IN2P3 (France); BMBF, DFG, and HGF (Germany); GSRT (Greece); OTKA and NKTH (Hungary); DAE and DST (India); IPM (Iran); SFI (Ireland); INFN (Italy); NRF (Korea); LAS (Lithuania); CINVESTAV, CONACYT, SEP, and UASLP-FAI (Mexico); PAEC (Pakistan); SCSR (Poland); FCT (Portugal); JINR (Armenia, Belarus, Georgia, Ukraine, Uzbekistan); MST and MAE (Russia); MSTDS (Serbia); MICINN and CPAN (Spain); Swiss Funding Agencies (Switzerland); NSC (Taipei); TUBITAK and TAEK (Turkey); STFC (United Kingdom); DOE and NSF (USA). Individuals have received support from the Marie-Curie IEF program (European Union); the Leventis Foundation; the A. P. Sloan Foundation; and the Alexander von Humboldt Foundation.

References

1 CMS Collaboration, "The CMS Experiment at the CERN LHC," JINST **3** S08004, 2008.
2 L. Evans and P. Bryant (editors), "LHC Machine," JINST **3** S08001, 2008.
3 CMS Collaboration, "Muon Technical Design Report," CERN-LHCC-97-32, 1997.

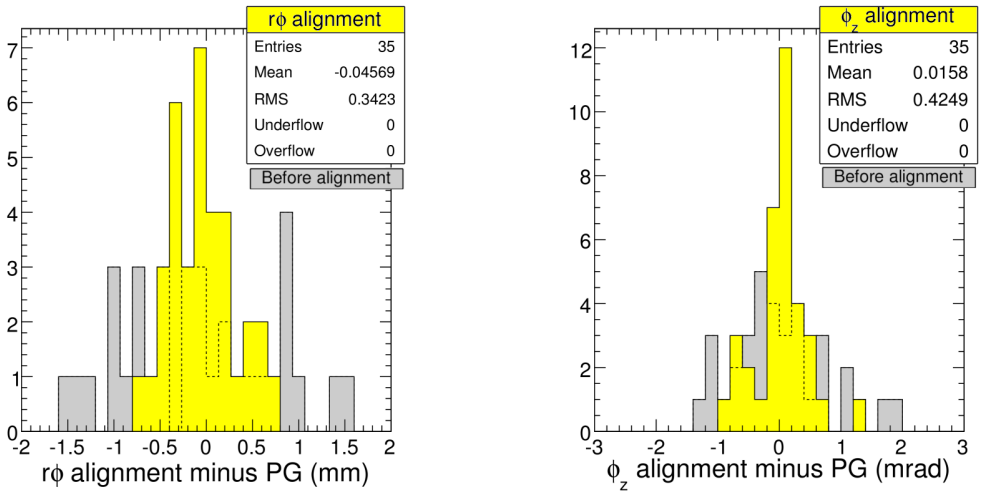

Figure 13: Histogram of aligned chamber parameters minus chamber parameters as measured by photogrammetry (PG).